# UNVEILING WALL SHEAR STRESS SPATIOTEMPORAL HETEROGENEITY IN CORONARY ARTERIES

**Karol Calò (1), Giuseppe De Nisco (1), Diego Gallo (1), Claudio Chiastra (1), Valentina Mazzi (1),
Ayla Hoogendoorn (2), Stefania Scarsoglio (3), David A. Steinman (4)
Jolanda J. Wentzel (2), Umberto Morbiducci (1)**

(1) Polito[BIO]Med Lab, Department of
Mechanical and Aerospace Engineering,
Politecnico di Torino,
Turin, Italy

(2) Department of Cardiology, Biomedical
Engineering,
Erasmus MC, 3000 CA Rotterdam,
The Netherlands

(3) Department of Mechanical and
Aerospace Engineering,
Politecnico di Torino, Turin, Italy

(4) Biomedical Simulation Lab, Department of
Mechanical & Industrial Engineering,
University of Toronto,
Toronto, Ontario, Canada

## INTRODUCTION

According to the "hemodynamic risk hypothesis" [1], low and oscillatory wall shear stress (WSS) contributes to the initiation of atherosclerosis [2]. However, fluid dynamics descriptors based only upon cycle-average WSS magnitude and/or direction do not fully capture the complex near-wall hemodynamic milieu [3], reinforcing the need for a more in-depth characterization of those WSS features involved in vascular disease onset/progression. Aiming at identifying more clearly the WSS features that promote arterial disease, here a dataset of ten personalized computational hemodynamic models of pig left anterior descending (LAD) coronary artery is considered [4]. On this dataset, correlation-based analysis and Complex Networks (CNs) theory are applied to the time-histories of WSS vector magnitude and of its "axial" and "secondary" components, according to a scheme recently applied to carotid bifurcation models [5]. Exploiting CNs ability to synthetically model the structure and function of complex physical systems, the study explores the spatiotemporal heterogeneity in the dynamics of the WSS along the cardiac cycle, at each point on the arterial wall. The main objective is to investigate if, besides the widely-recognized atheroprone action of low WSS magnitude on endothelial cells (EC), also the shape of WSS time-histories along the cardiac cycle may be involved in the biological events triggering coronary atherosclerosis.

## METHODS

An overview of the methods is provided in **Fig.1**. The LAD of ten ostensibly healthy adult mini-pigs was imaged by computed coronary tomography angiography (CCTA) and intravascular ultrasound (IVUS), and flow-rates at inflow and outflow boundaries were derived from local Doppler-based velocity measurements. On the reconstructed models, unsteady-state computational fluid dynamics (CFD) simulations were performed, based on the finite-volume method. Extensive details on methods are provided elsewhere [4]. Side branches were removed in the post-processing steps and the spatiotemporal analysis was performed on
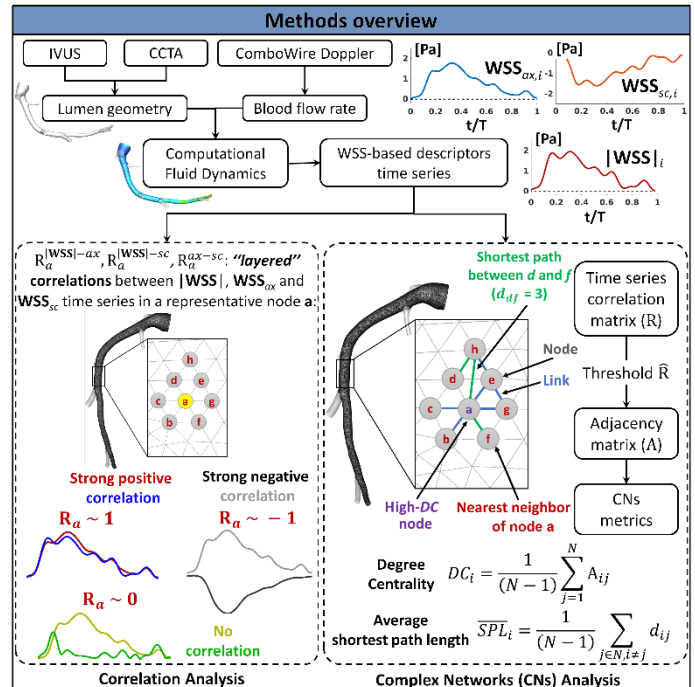


**Figure 1: Overview of the methods. Examples of correlations between time series and a schematic representation of a CN are also provided. T: period of the cardiac cycle; *N*: n° of grid nodes.**

three hemodynamic descriptors computed on the main vessel: the WSS magnitude (|**WSS**|), its "axial" component (**WSS**$_{ax}$) tangent to the local vessel centerline and related to the main flow direction, and its "secondary" component (**WSS**$_{sc}$), perpendicular to **WSS**$_{ax}$ and related to secondary flows [6]. *"Layered"* correlations were computed between the time series of such quantities along the cardiac cycle at each node $i$ of the wall superficial mesh, using the following Pearson correlation coefficients: $R_i^{|WSS|-ax}$ (magnitude *vs.* axial time series), $R_i^{|WSS|-sc}$ (magnitude *vs.* secondary), and $R_i^{ax-sc}$ (axial *vs.* secondary).

On each LAD model, three CNs were built, one for each WSS-based descriptor time series considered to study WSS spatiotemporal heterogeneity. In detail, in the CNs the nodes are represented by the time series at the grid points of the surface mesh, and two nodes of the network are connected by a topological link $\{i, j\}$ if the Pearson correlation $R_{ij}$ between the time series at nodes $i$ and $j$ is greater than a set threshold value $\hat{R}$ [5]. Each CN is represented by its adjacency matrix $A_{ij}$ containing all the information about node connectivity: $A_{ij} = 1$ if a link exists between nodes $i$ and $j$ ($R_{ij} > \hat{R}$), $A_{ij} = 0$ elsewhere. Two metrics were computed to characterize the structure of the CNs: (1) the *degree centrality* ($DC_i$) of node $i$, defined as the percentage of nodes of the CN connected to node $i$ (the "nearest neighbors" of $i$, **Fig. 1**); (2) the *average shortest path length* ($\overline{SPL}_i$) of node $i$, quantifying the average length of the shortest paths $d_{in}$ connecting node $i$ and any other node $n$ in the CN. $DC$ and $\overline{SPL}$ measure, respectively, the homogeneity/heterogeneity of each surface node WSS-based quantity time series with respect to the whole luminal surface, and the topological length of the correlation persistence (i.e., the smaller the $\overline{SPL}_i$, the larger the persistence length of the correlation between $i$ and the rest of the CN).

## RESULTS

The luminal distributions of the *"layered"* correlations are displayed in **Fig. 2A** for the explanatory LAD model B. As a general observation common to all the LAD models, the |**WSS**| and **WSS**$_{ax}$ time-histories at each node are strongly correlated (>0.9, **Fig. 2A** left panel). This emergent feature, together with the observed very similar distributions of the cycle-average |**WSS**| and **WSS**$_{ax}$ (**Fig.2D** left and middle panels) confirms that WSS is predominantly aligned with the axial direction in the LAD. The maps of the *"layered"* correlations with **WSS**$_{sc}$ (**Fig.2A** middle and right panels) reflect the luminal distribution of the cycle-average **WSS**$_{sc}$ (**Fig.2D** right panel), characterized by the presence of positive and negative (right-/left-handed) secondary components. For $R_i^{ax-sc}$, this is like saying that the hemodynamics in the LAD causes the secondary and the axial WSS to be either "in phase" (strong positive correlation, **Fig.1**) or "out-of-phase" (strong negative correlation, **Fig.1**) on the luminal surface.
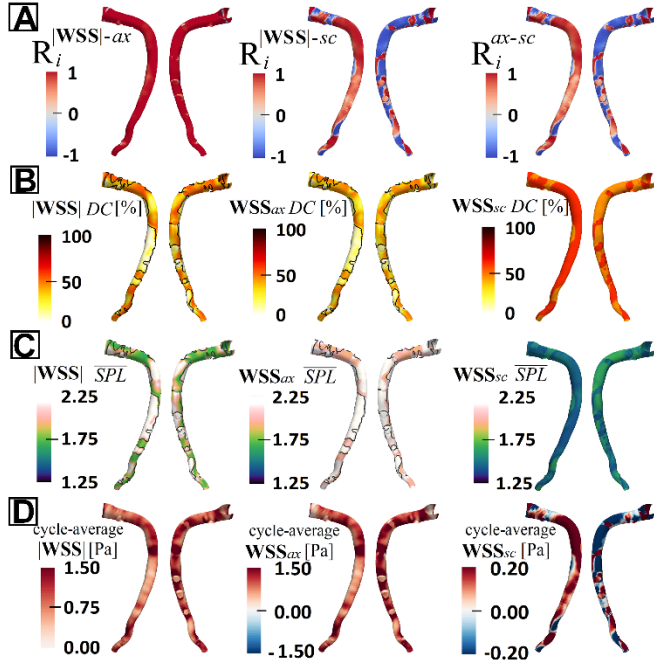
The results of the CNs analysis on the explanatory model B are reported in **Fig.2B** and **2C**. As expected, |**WSS**| and **WSS**$_{ax}$ CNs have almost identical topological structures (**Fig.2B** left and middle panels), with low $DC$ regions mainly located at the inner wall. Interestingly, such low $DC$ regions, where the WSS time-histories are the least representative of the whole network (i.e., of the WSS waveforms shape), co-localize very well with the luminal surface areas exposed to low cycle-average |**WSS**| (black contour lines in **Fig.2B**). The $DC$ maps of **WSS**$_{sc}$ (**Fig.2B**, right panel) reflect the presence of opposite-signed secondary components characterizing WSS directionality, giving rise to two large regions of medium/high $DC$ (around 35% and 65%), where **WSS**$_{sc}$ waveform shapes are more similar. Lastly, the $\overline{SPL}$ luminal distributions of |**WSS**| and **WSS**$_{ax}$ CNs are, in general, similar, with the displayed model B being the one in the dataset presenting the most evident, albeit modest, differences (**Fig.2C** left and middle panels). In general, it emerges that in some regions at the inner wall |**WSS**| and **WSS**$_{ax}$ waveforms are separated by the rest of the nodes by at least 2.25 topological links, exhibiting the shortest length of correlation persistence (highest $\overline{SPL}$ values). Those high $\overline{SPL}$ value regions markedly co-localize with low cycle-average |**WSS**| regions (white contour lines in **Fig.2C**). As for the **WSS**$_{sc}$ CNs, they exhibit a less pronounced inter-variability in terms of $\overline{SPL}$, with shorter topological paths ($\overline{SPL}$=1.5 on average, **Fig.2C** right panel) and, subsequently, a more marked persistence of the spatiotemporal correlations.

## DISCUSSION

Here a correlation + CN-based approach is proposed to investigate WSS spatiotemporal heterogeneity in coronary arteries. Differently from the classical approach, in which only integral (i.e., cycle-average) WSS-based descriptors are considered, here WSS waveforms along the cardiac cycle are investigated, and dynamically correlated WSS patterns are identified and characterized. The present findings suggest that where the WSS is low in magnitude, the time-histories of WSS-based descriptors are markedly different in shape from elsewhere in the vessel and have a short topological correlation length, consistently with previous studies on the distinct modulation of EC phenotype in response to "atheroprone" and "atheroprotective" WSS waveforms [7]. This implies that not only the magnitude of the cycle-average WSS [1, 2], but also the shape of WSS waveforms along the cardiac cycle, may induce mechanobiological responses on EC, contributing to trigger atherosclerosis at its earliest stage.



**Figure 2: Luminal distributions of: A) *"Layered"* correlations; B) $DC$; C) $\overline{SPL}$; D) cycle-average |WSS|, WSS$_{ax}$ and WSS$_{sc}$, for the explanatory model B. Black contour lines in B) and C) delimit low cycle-average |WSS| surface areas.**

## REFERENCES

[1] Morbiducci, U et al., *Thromb Haemost*, 115(3):484-92, 2016.
[2] Ku, DN et al., *Ultrasound Med Biol,* 11(1):13-26, 1985.
[3] Gallo, D et al., *J R Soc Interface,* 15:20180352, 2018.
[4] De Nisco, G et al., *Ann Biomed Eng,* 47(2):425-438, 2019.
[5] Calò, K et al., *IEEE TBioMedEng,* 10.1109/TBME.2019.2949148
[6] Morbiducci, U et al., *J Biomech,* 48(6):899-906, 2015.
[7] Dai, G et al., *PNAS,* 101(41):14871-14876, 2004.